AD 42856

UNCLASSIFIED

PRINCETON UNIVERSITY

DEPARTMENT OF AERONAUTICAL ENGINEERING

DEPARTMENT OF THE NAVY
BUREAU OF AERONAUTICS

Contract Noas 53-817-c

COMBUSTION INSTABILITY

IN

LIQUID PROPELLANT ROCKET MOTORS

Eighth Quarterly Progress Report

For the Period 1 February 1954 to 30 April 1954

Aeronautical Engineering Report No. 216-h

Prepared by Jerry Grey
J. Grey, Research Engineer

Approved by Jerry Grey
L. Crocco, Professor in Charge
for

1 June 1954

PRINCETON UNIVERSITY

Department of Aeronautical Engineering

CONTENTS

	Page
TITLE PAGE	1
CONTENTS	2
I. SUMMARY	3
II. INTRODUCTION	4
A. Object	4
B. History	5
III. THEORY	9
IV. APPARATUS	9
A. Monopropellant Rocket Motor	9
B. Bipropellant Rocket Motor	10
C. Instrumentation	12
APPENDIX A: Derivation of Pressure-Velocity Phase Difference for Monopropellant Swirl Injector	21

1. SUMMARY

A pump-pressurized cooling system for the bipropellant rocket motor nozzle has been constructed and calibrated. Shakedown tests were performed under steady-state conditions at a chamber pressure of 600 psi, and results are, in general, satisfactory. A small crack observed in the 300 psi injector face, used on the last series of runs, appears to be due to a stress concentration and has been corrected in subsequent injectors by the use of relieving fillets. No other damage has occurred on any of the bipropellant system components.

Steady state water flow calibrations were performed on the cavitating venturis, 300 and 600 psi injectors, and existing flow modulating unit pistons. These tests have been used to establish the limits of operation of the various components in conjunction with each other, and will be used for determination of proper settings and test conditions for forthcoming tests with flow modulation.

Development has continued on the hot-wire flow phasemeter probe and amplifier, and a number of different type probes have been tested for sensitivity and application to the type of flow encountered on these tests. Additional development work on the amplifier has removed all inherent phase shift from the system and has been successful in providing flat frequency response in the range required. A method for determining the response of the hot wire when used in the system configuration with the flow-modulating unit has been designed and built. This apparatus will permit detection of any inherent phase lag introduced by the hot wire itself.

Refinement of the instrumentation system is nearly complete. All major components have been checked with the exception of the cathode followers, filters, and phase-measuring device which are to be used for the dynamic records. Checkout of the constant-phase amplifiers and tape recorder revealed the necessity for a low-frequency end phase shift network and an additional output attenuator on the amplifiers, and phase compensation was necessary on the Ampex tape recorder. These two components now perform satisfactorily on all four channels. As reported previously, all of the transmission line systems and mean value recording systems are operating satisfactorily within the maximum permissible errors as required.

The Li-Liu pressure pickups are now in current use on the bipropellant chamber, and apparently are performing satisfactorily in all respects except for what appears to be a small amount of temperature drift, which, however, is apparently quite predictable.

II. INTRODUCTION

A. Object

ButAer Contract NOas 52-713-c was undertaken as a part of the jet propulsion research program of the Department of Aeronautical Engineering at Princeton to "conduct an investigation of the general problem of combustion instability in liquid propellant rocket engines." This program shall consist of theoretical analyses and experimental verification of theory. The ultimate objective shall be the collection

of sufficient data that shall permit the rocket engine designer to produce power plants which are relatively free of the phenomena of instability. Interest shall center in that form of unstable operation which is characterized by high frequency vibrations and is commonly known as "screaming."

B. History

Interest at Princeton in the problem of combustion instability in liquid propellant rocket motors was given impetus by a Bureau of Aeronautics symposium held at the Naval Research Laboratory on the 7th and 8th of December 1950. This interest resulted in theoretical analyses by Professors M. Summerfield and L. Crocco of this Center.

Professor Summerfield's work, "Theory of Unstable Combustion in Liquid Propellant Rocket Systems" (JARS, September 1951), considered the effects of both inertia in the liquid propellant feed lines and combustion chamber capacitance with a constant combustion time lag, and applied to the case of low (up to about [illegible] cycles per second) frequency oscillations sometimes called "chugging."

Professor Crocco advanced the concept of the pressure dependence of time lag in mid-1951; his paper "Aspects of Combustion Stability in Liquid Propellant Rocket Motors" (JARS, November 1951 and Jan.-Feb. 1952), presents the fundamentals resulting from this concept, and analyzes the cases of low frequency instability with monopropellants, low frequency instability with bipropellants and high frequency instability, with combustion concentrated at the end of the combustion chamber.

Desiring to submit the concept of a pressure dependent time lag to experimental test, a preliminary proposal was made by the University to the Bureau of Aeronautics in the summer of 1951, and following a formal

request, a revised proposal was submitted which resulted in Contract NOas 52-713-c.

Analytical studies with concentrated and distributed combustion had been carried on in the meantime under Professor Crocco's direction and within the sponsorship of the Guggenheim Jet Propulsion Center by S. I. Cheng and were issued as his Ph.D. thesis, "Intrinsic High Frequency Combustion Instability in a Liquid Propellant Rocket Motor," dated April 1952.

Time was devoted, in anticipation of the contract, during the first third of 1952, to constructing facilities, securing personnel, and planning the experimental approach.

During the first three month period of the contract year, personnel and facilities at the new James Forrestal Research Center were assigned, and the initial phases of the experimental program were planned in some detail.

A constant rate monopropellant feed system was designed and preliminary designs of the ethylene oxide rocket motor and the instrumentation systems were worked out. Special features of the projected systems included a flow modulating unit to cause oscillations in propellant flow rate, a water-cooled strain-gage pressure pickup designed for flush mounting in the rocket chamber, and several possible methods for dynamic measurement of an oscillating propellant flow rate.

Searches were made of the literature for sources of information on combustion instability and ethylene oxide, and visits to a number of activities working on liquid propellant rocket combustion instability problems were made for purposes of familiarization with equipment and results.

The basic precepts of Crocco's theory for combustion instability were reviewed, and detailed analyses made for specific patterns of combustion

[illegible]

Operational tests and calibration of the Princeton-MIT pressure pickup proved the value of the design, although failure of the pickup under "screaming" rocket conditions showed the necessity for modification of the cooling system.

Construction of the monopropellant test stand and rocket motor was completed. Modifications were made to the Princeton-MIT pressure pickup to provide for higher permissible heat-transfer rates in order that it be satisfactory for use under "screaming" conditions in a bipropellant rocket motor. Construction and preliminary testing of the hot-wire flow phasemeter and its associated equipment were completed.

A new contract, NOas 53-817-c, dated 1 March 1953, was granted by the Bureau of Aeronautics to continue the program originally started under NOas 52-713-c. Operation of the monopropellant rocket motor was begun under this new contract, and shakedown operations were completed. It was found that decomposition of ethylene oxide could not be attained with the original motor design despite many configuration changes, and it was decided to avoid a long and costly development program by operating the "monopropellant" motor with small amounts of gaseous oxygen. The required limits of oxygen flow rate were determined at several chamber pressures, and it was demonstrated that the oxygen would probably have a negligible effect on performance when compared to the effect of ethylene oxide flow rate modulation. Preliminary tests with flow rate modulation up to 100 cps were performed for the purposes of system checkout, using interim AC amplifiers in lieu of the necessary DC instruments.

The time constant of the hot-wire liquid flow phasemeter was found to be 0.15 milliseconds and preparations for instantaneous flow

calibrations were made. A test rig was constructed for this purpose.

A bipropellant rocket system using liquid oxygen and 100% ethyl alcohol was designed on the basis of monopropellant operational experience, incorporating an adjustable phase flow modulating unit on both propellants. Injector design was based on a configuration used extensively by Reaction Motors, Inc.

Operation of the monopropellant system was performed with flow modulation at frequencies up to 120 cps, using a composite instrumentation system to measure mean values, amplitudes of oscillation, and phase difference between injector and chamber pressures. Analysis of the results of this program demonstrated approximate adherence to the pressure-time lag relationship used in Crocco's original theoretical treatment. Accuracy of the measurements was not adequate to provide a detailed check of the theory, however, so an instrument refinement and development program was initiated.

The Mittelman electromagnetic flowmeter proved unsatisfactory due to equipment malfunctions, and had to be abandoned as a possible means of measuring instantaneous flow rates. The Li dynamic flowmeter also experienced a number of mechanical failures, and it was decided to concentrate all flow-measurement effort on the hot-wire, which, of all flowmeters tested, appeared to show the most promising results.

Shakedown operation of the bipropellant rocket chamber at 300 psi was completed and steady state mixture-ratio tests were run satisfactorily. All components of the bipropellant test stand were checked out including the flow modulating unit, which was operated at speeds up to 12,000 RPM. Progress of the instrumentation refining program was satisfactory with the mean value recording system and the transmission line networks providing

satisfactory operating accuracy.

Subsequent efforts are presented in detail in the present report.

III. THEORY

A theoretical analysis of the phase lag between pressure and flow rate perturbations in the swirl-type monopropellant injectors was made. This analysis illustrates the fact that the necessary corrections to the recorded pressure drop oscillations across the injector in order to obtain the instantaneous flow rate are appreciable.

Axially-symmetric flow of an incompressible fluid is assumed in order to reproduce analytically the flow through the swirl type injectors. The results indicate that there exist both a phase lag and an amplitude ratio between perturbations in pressure drop and flow rate. As would be expected, these effects increase with increasing flow modulation frequency, but decrease with increasing mean flow rates. The results demonstrate, however, that these effects are of sufficient order of magnitude that they must be taken into account in any analysis which attempts to relate the time lag to measurements of the pressure drop across the injector. Until such time as hot-wire tests are available for making experimental checks on this analysis, the theoretical results will be used directly for computations of the combustion time lag in the monopropellant rocket motor. Details of the analysis appear in Appendix A of the present report. A similar analysis will be made for the bipropellant injector.

IV. APPARATUS

A. Monopropellant Rocket Motor

The monopropellant rocket motor has been used during this report

period primarily as a vehicle for tests on the hot-wire flow phenomena. An indexing device to be used in determinations of the probe response time has been mounted on the shaft of the monopropellant flow modulating unit. This device will be discussed below at some length under "Instrumentation."

B. Bipropellant Rocket Motor

A nozzle coolant pump and its drive motor have been installed on the bipropellant test stand in order to supply adequate cooling for the rocket nozzle. This installation is shown in Figure 1. A 7½ HP induction motor rotating at 1725 RPM is used to drive a hydraulic gear pump with a rated capacity of 15 gallons per minute at 1200 RPM and 1000 psi. Two Fluid Controls, Inc. relief valves are installed on the pump outlet, one for use in setting the required coolant pressure, the other to act as a safety overload relief in case the nozzle coolant passages should become obstructed. The operating condition of the cooling system has been set at 400 psi nozzle coolant inlet pressure and 100 psi outlet pressure, with a coolant flow in the present nozzle of approximately 1 pound per second. Provision has been made to double this coolant flow by increasing nozzle coolant passage inlet and outlet areas for tests at higher chamber pressures, but the present flow rate is theoretically capable of permitting heat transfer rates through the copper nozzle up to at least 4 Btu per square inch per second without damage to the nozzle.

After disassembly of the chamber due to the burned nozzle described in the last Quarterly Progress Report, careful examination of the 300 psi injector revealed a hairline crack in the injector face running completely around the apex of the V-groove which forms the exit surfaces of the impinging jet orifices. The crack was apparently due to stress

concentrations induced by thermal shock to the V-groove apex, and a new 300 psi injector was fabricated with a rounded apex to relieve this condition. The nature of the crack is shown in Figure 2. Unfortunately the first 600 psi injector had been fabricated prior to noticing of the crack in the 300 psi injector, and, it is consequently being used with extreme care, a detailed inspection of its surface being made after each run. Meanwhile, a new stress-relieved 600 psi injector is being manufactured to replace it at the earliest possible time.

Prior to continuing the rocket motor tests, a series of water flow calibrations of both 300 and 600 psi bipropellant components was made to establish the operating limits of the cavitating venturis in conjunction with the flow modulating unit. This was done in order to establish that the pressure oscillations introduced by the flow modulating unit did not exceed the operating limits of the venturis or, on the other hand, cause the injection pressure to drop below the chamber pressure. Tests were run with a single set of pistons, both sets of cavitating venturis, and both 300 and 600 psi injectors. The limit curves for this single set of pistons were drawn up and the required operating system pressures selected for both steady-state tests and tests with flow modulation.

Shakedown testing of the bipropellant system with alcohol and liquid oxygen was satisfactorily concluded at 600 psi chamber pressure, and preparations were made for beginning hot tests with flow modulation at both 300 and 600 psi chamber pressure with a single set of bipropellant flow modulating pistons. Pistons of additional diameters for other ranges of modulating frequency will not be put into manufacture until the theoretical determination of the proper piston size is confirmed on these forthcoming tests.

C. Instrumentation

The basic recording system to be used on monopropellant and bipropellant tests is now complete. Calibration techniques and system checkout methods have been established both for mean value components, as indicated in the last report, and also for the oscillating portions of the significant signals. The transient data recording system, consisting of constant phase AC amplifiers, a four channel preamplifier, the four channel Ampex recorder, four channels of a cathode follower for matching the tape recorder output to the recording oscillograph, and the oscillograph itself have been checked out in considerable detail. A number of adjustments were [illegible]. For example, it was found that the noise level would be markedly [illegible] by using the constant phase amplifiers at their maximum possible [illegible] and introducing attenuation between the amplifier and the tape [illegible]. A low-frequency and phase shift network was found to be necessary [illegible] these amplifiers in order to permit operation as low as 10 cycles per second, and phase compensation was necessary on the Ampex tape recorder [illegible] demodulator. Full calibrations of the entire system indicate that [illegible] of the order of 1 to 2% are possible both with respect to amplitude and constancy of the phase of a signal.

Completion of Central Recording Room revisions is approaching, and modifications have reached the point at which full scale testing may be accomplished without impediment. Photographs of the revised Central Recording Room layout are included in Figures 3 and 4, showing the full patch-panel arrangement for transmitting data from the test cells to the various pieces of equipment. The convenient arrangement of steady state and transient recording instruments has resulted in highly improved efficiency of operation of the instruments and reduction of personnel error in recording the data.

Intensive development on the hot wire flow phasemeter was carried out during this report period. Different designs of probe were experimented with in attempting to determine the optimum configuration for measuring the fairly high frequency oscillations in the high energy liquid line at high pressures. The originally considered nickel probe of .002-inch diameter was found to be of insufficient sensitivity when used in short lengths. It was found necessary to use rather long pieces of nickel wire in the form of a multiwired grid wound around a pair of supports in order to obtain sufficient resistance for the required sensitivity. Experiments to improve this situation were made with a glass filament coated with a sputtered film of tungsten whose thickness could be controlled so as to control the resistance and hence the sensitivity of the probe at will. Unfortunately, probes fabricated using this technique proved both expensive and too delicate for practical operation. A change was made from the glass filament to a silica filament .001 inches in diameter, and instead of tungsten, the silica filament was plated with a controlled thickness of nickel. Resistances in the proper range were obtained by the use of a carefully controlled plating process, and this type of probe is now being readied for insertion inside one of the monopropellant injectors. Meanwhile a number of tests were run on the monopropellant test stand using a large "workhorse" probe in conjunction with the monopropellant pulsing unit in order to check out all features of the bridge, amplifier and transmission system. The probe used here was one of the grid-wound multiwired nickel probes with resistance in the range to provide signals adequate for test work.

This probe was mounted in a straight pipe in the feed line at the approximate location of the rocket motor, and water tests with flow modulation were performed in order to establish wire operating temperatures

and frequency range of the system.

The indexing device mentioned earlier will be used during the forthcoming report period to establish the response time of the probe under its expected operating conditions in the following way. A large stainless steel disc containing a very small magnet at its outer edge has been mounted on the shaft of the monopropellant flow modulating unit. A pickup coil mounted on the thrust stand itself produces a signal every time the magnet, which is located at the top-dead-center position of the flow modulating piston, passes the coil. Thus, the elapsed time between the indexing mark and a characteristic point of the hot-wire trace may be measured. When this is done at a number of modulating frequencies, this measured value of the elapsed time should be essentially constant, regardless of the frequency. If this is actually the case, then the response time of the hot wire is sufficiently rapid that it may be assumed to respond instantaneously to oscillations up to the maximum operating frequency of the flow modulating unit. These tests are being made to corroborate under simulated test conditions the results published last year which described the effects of introducing a step function into the flow past one of the older models of the hot-wire flow phasometer.

Once these final response-time checks have been concluded, calibrations of the relationship between instantaneous flow and pressure drop across the monopropellant injector orifices will be made to check the theoretical analysis included as Appendix A to the present report.

Calibrations of the latest shipment of Li-Liu pressure pickups have been completed. It was found that hysteresis of the differential-type pickups could be reduced to a negligible value if the pickup reference pressure was never allowed to exceed the pressure to be measured, and provision

for operating the pickups under these conditions has been made on both test stands. Calibration tests of all pickups now on hand indicate that the required degree of accuracy may be obtained repeatedly on the majority of the pickups. As mentioned in the previous Quarterly Progress Report, however, one major factor which still remains to be observed with some degree of care is the effect of temperature upon these pickups when used in typical rocket test operations. These tests have been begun by observing the amount of zero drift occurring on some of the bipropellant rocket motor tests. The method of operating the present rocket chamber, using extended periods of liquid oxygen precooling in order to avoid vaporization of oxygen in the injector at the time the propellant valve is opened, [illegible] the pressure pickups to extreme temperature differentials over a [illegible] short period of time. The pickups are required to go from [illegible] comparable to that of liquid oxygen to typical rocket combustion [illegible] within a period of several seconds, and a small amount [illegible] drift has been observed. Provision has been made to determine this [illegible] in some detail by the use of a "control" pickup [illegible] some distance from the chamber, but sensing the same steady-state [illegible] as does the pickup mounted directly in the manifold. The length [illegible] introduced here has very little effect upon the steady state component [illegible] being measured, particularly if this determination is made [illegible] conditions of steady state operation of the chamber. These tests will [illegible] concurrently with the forthcoming series of runs with flow [illegible].

The temperature effect will also be investigated at the NACA under equilibrium conditions in cooled rocket chambers to determine whether the temperature drift is a transient effect or whether conditions of equilibrium

can be [illegible]. These tests are also expected to establish whether or not the [illegible] provisions of the present pickup are adequate for higher rates of heat transfer and for long periods of operation as well as for the short tests already made.

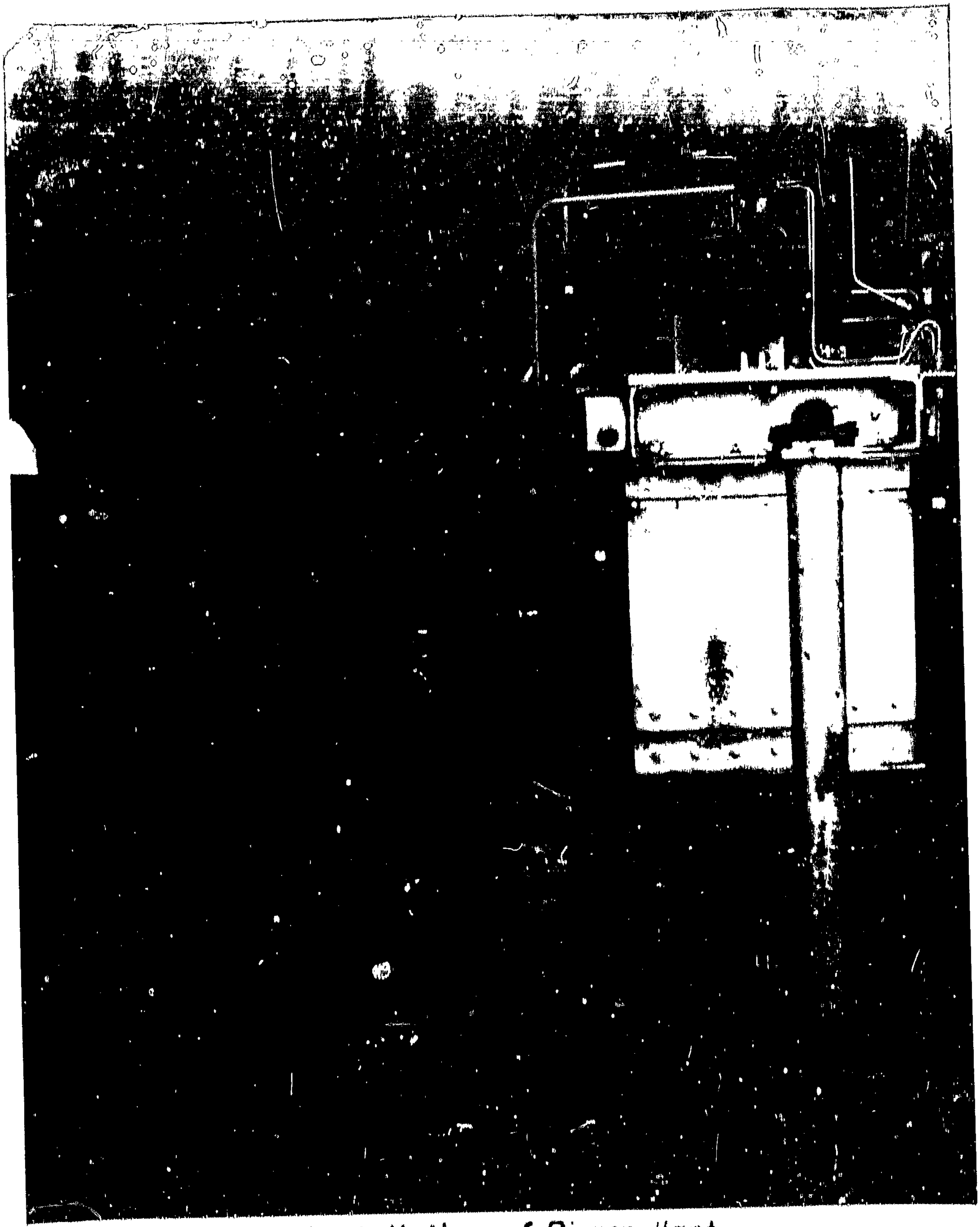

Figure I Installation of Bipropellant
Nozzle Coolant Pump and
Relief Valves

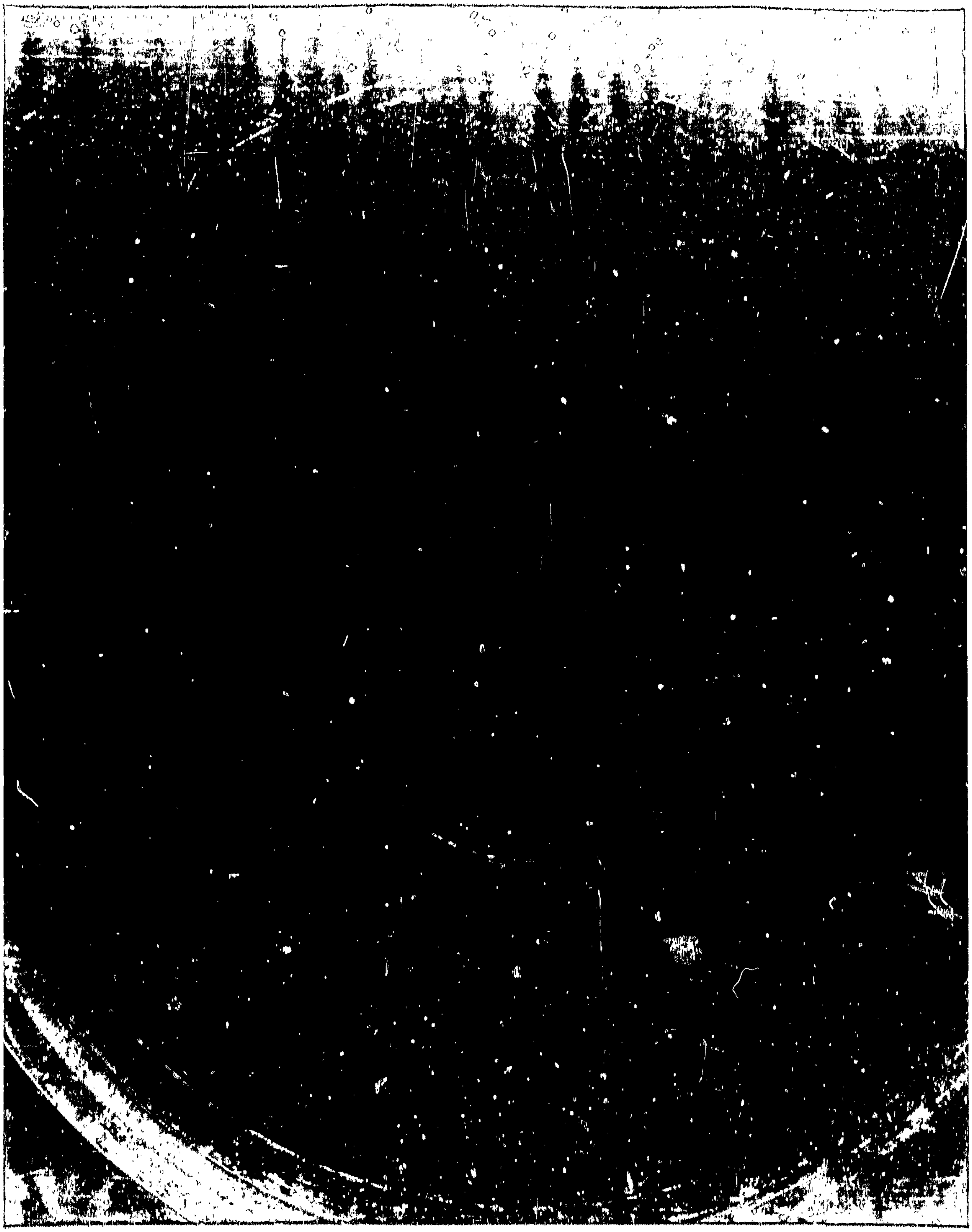

Figure 2 Crack in 300psi Bipropellant Injector, as a Result of Stress Concentrations

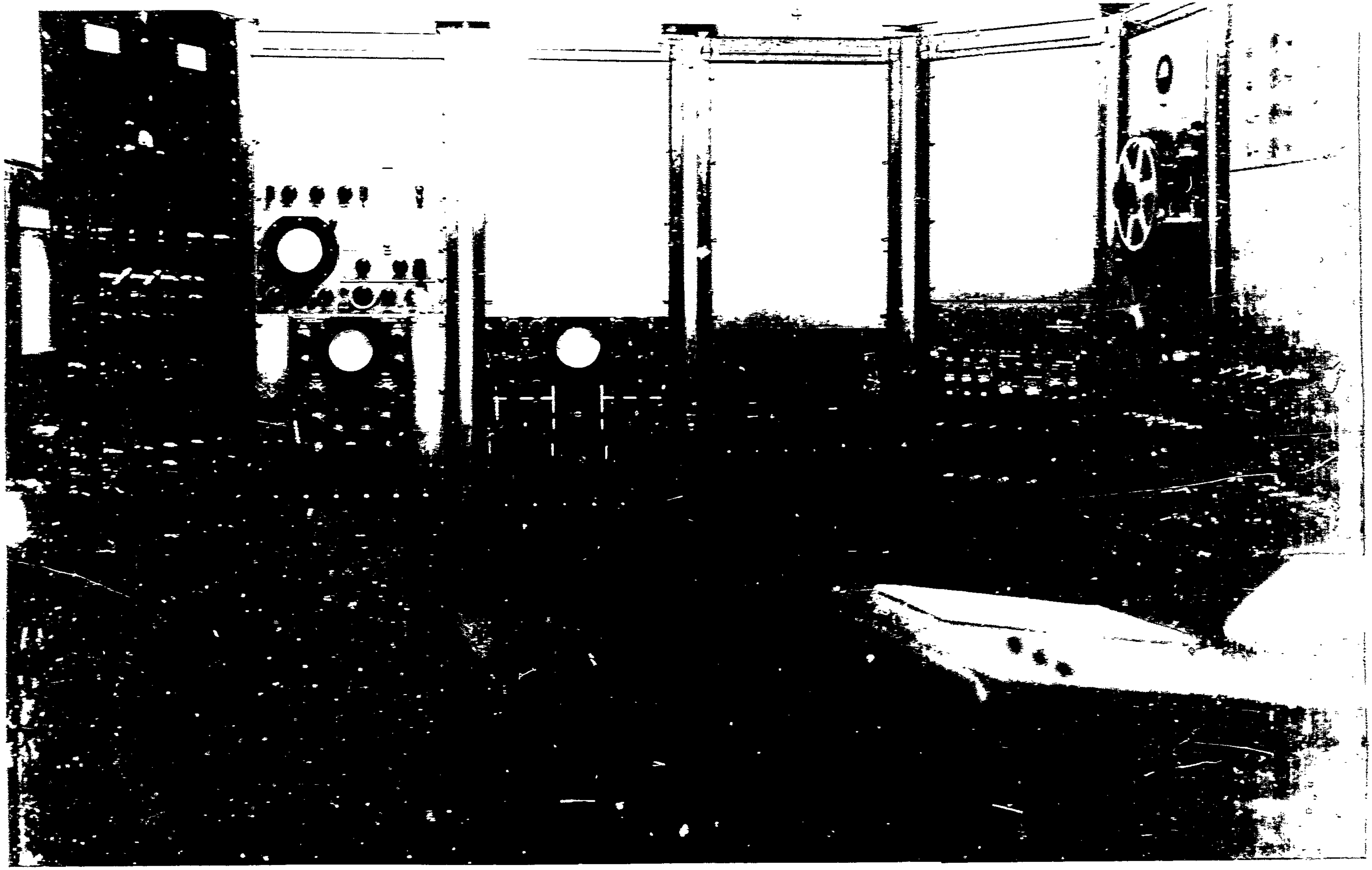

Figure 3: New Layout of Central Recording Room, Showing Transient Instrumentation

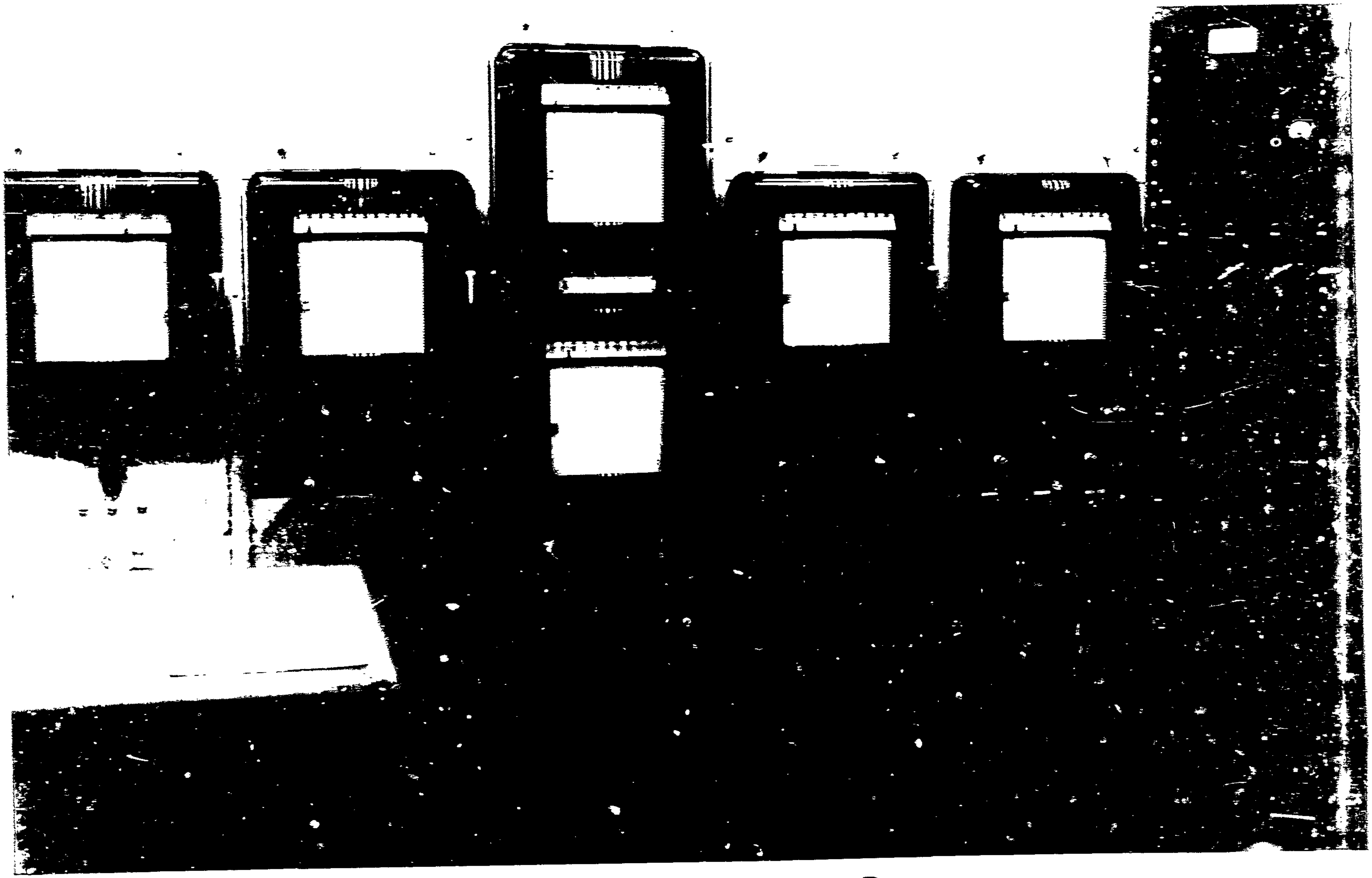

Figure 4. New Layout of Central Recording Room, Showing Steady-State Instrumentation

APPENDIX A

DERIVATION OF PRESSURE-VELOCITY PHASE DIFFERENCE FOR MONOPROPELLANT SWIRL INJECTOR

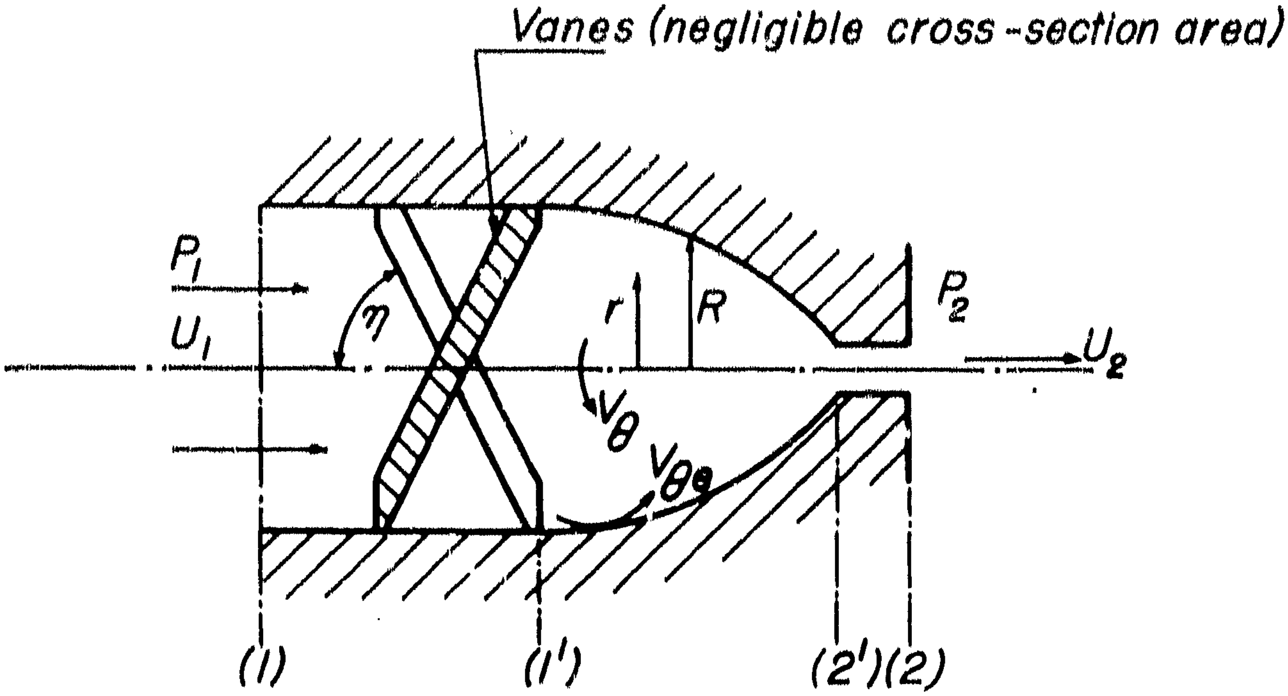

Figure 1: Diagram of Monopropellant Injector.

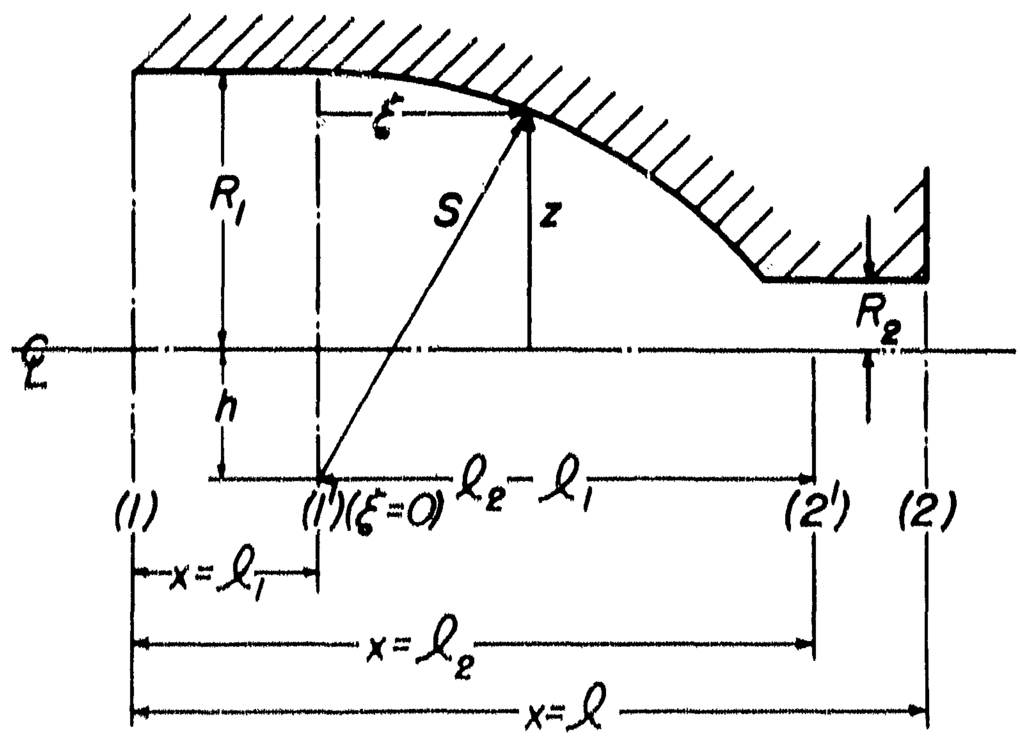

Figure 2: Monopropellant Injector Showing Details of Notation Used.

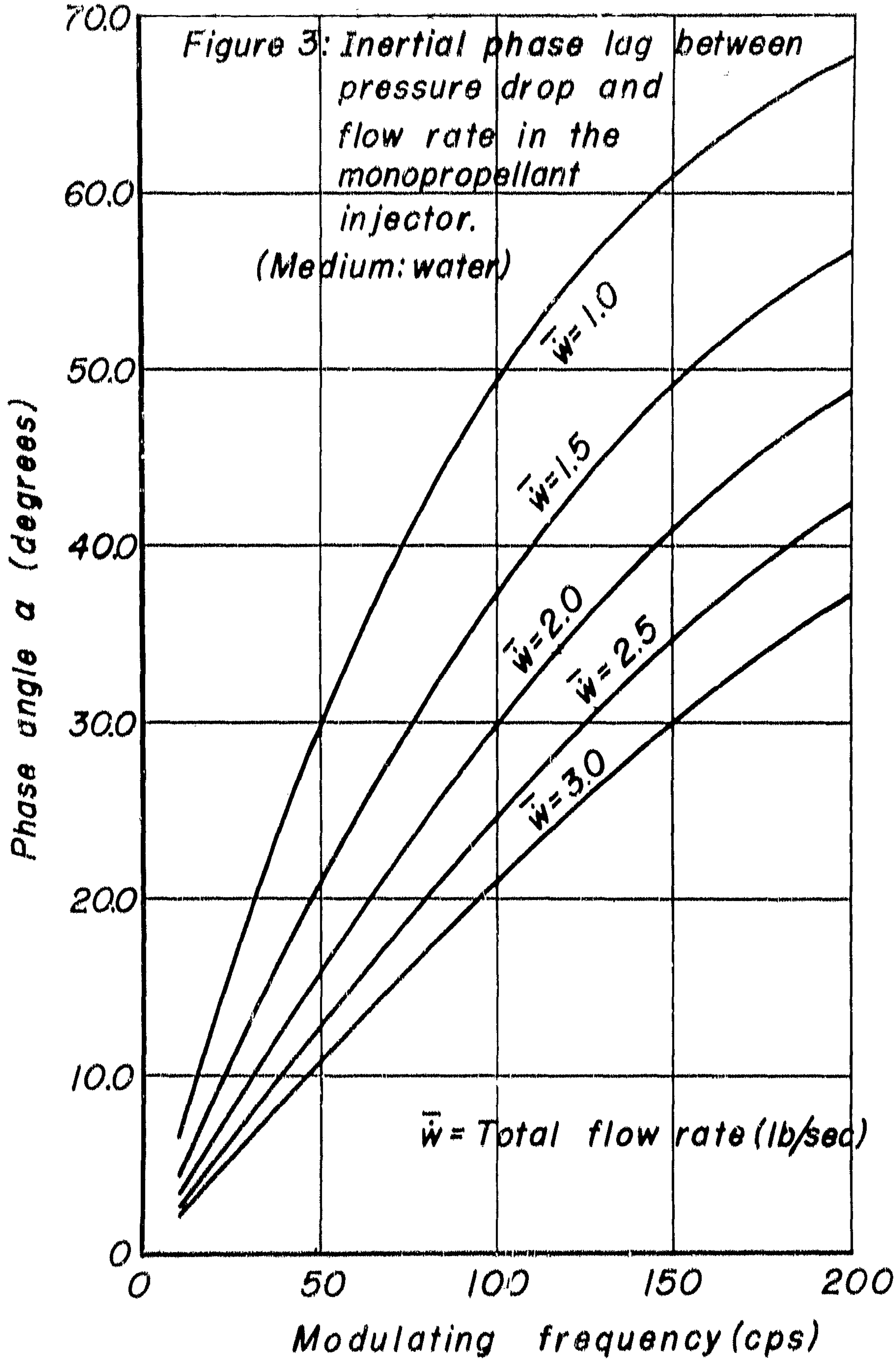
Figure 3: Inertial phase lag between pressure drop and flow rate in the monopropellant injector.
(Medium: water)
$\bar{\dot{w}}$=1.0
$\bar{\dot{w}}$=1.5
$\bar{\dot{w}}$=2.0
$\bar{\dot{w}}$=2.5
$\bar{\dot{w}}$=3.0
$\bar{\dot{w}}$ = Total flow rate (lb/sec)
Phase angle a (degrees)
Modulating frequency (cps)
0
10.0
20.0
30.0
40.0
50.0
60.0
70.0
0
50
100
150
200

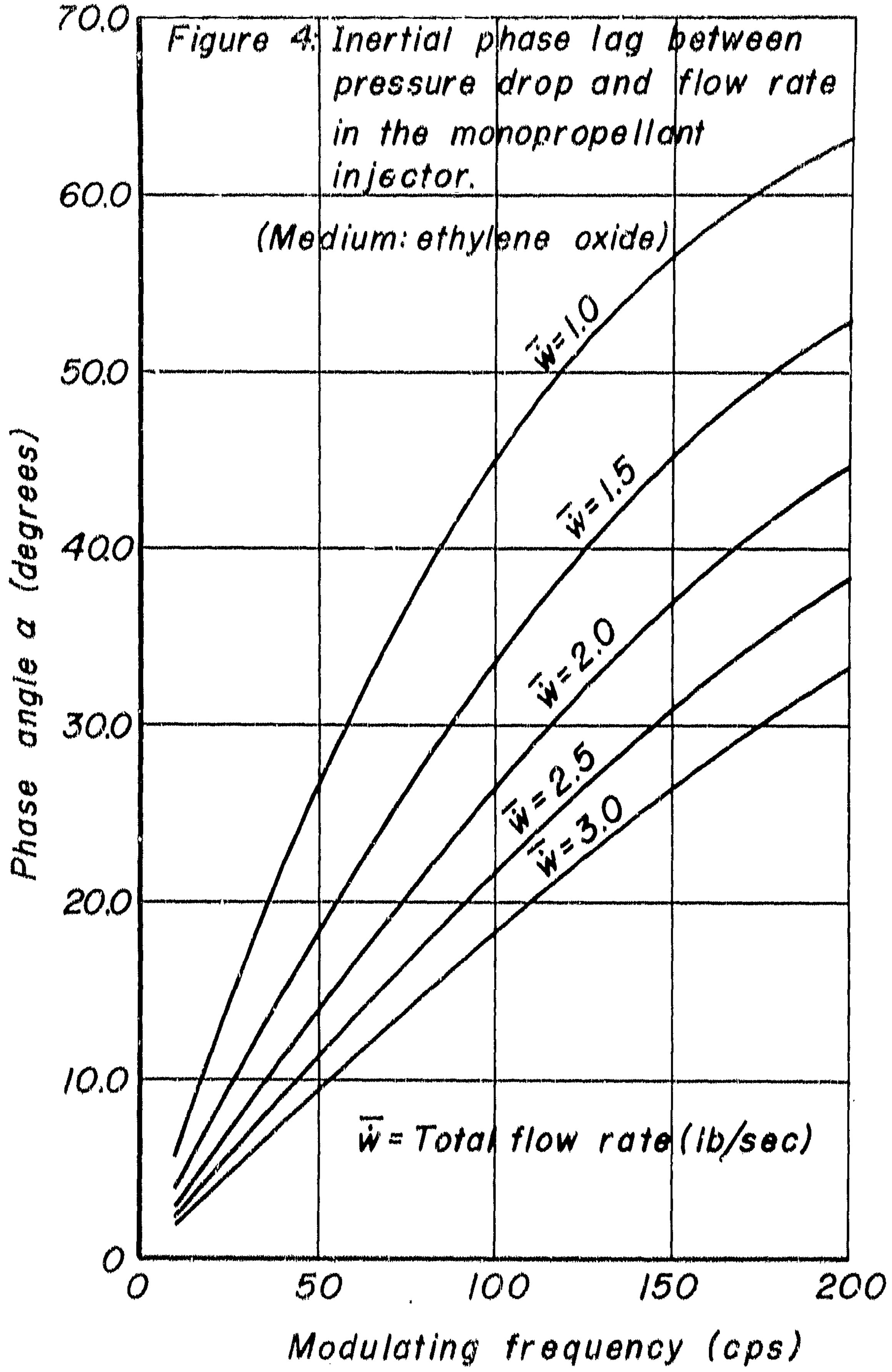
Figure 4: Inertial phase lag between pressure drop and flow rate in the monopropellant injector.
(Medium: ethylene oxide)
Phase angle α (degrees)
Modulating frequency (cps)
ẇ = Total flow rate (lb/sec)
ẇ=1.0
ẇ=1.5
ẇ=2.0
ẇ=2.5
ẇ=3.0
70.0
60.0
50.0
40.0
30.0
20.0
10.0
0
0
50
100
150
200

Derivation of Pressure-Velocity Phase Difference for Monopropellant Swirl Injector

Assumptions:

1. Flow is axially symmetric
2. Fluid is non-viscous and incompressible

In polar coordinates (cylindrical), the equations for incompressible flow become (with no variation of quantities in angular direction because of axial symmetry):

a. Continuity –

$$\frac{1}{r}\frac{\partial}{\partial r}(r V_r) + \frac{\partial u}{\partial x} = 0$$

b. X-directed Momentum –

$$\frac{\partial u}{\partial t} + u\frac{\partial u}{\partial x} + V_r\frac{\partial u}{\partial r} = -\frac{1}{\rho}\frac{\partial P}{\partial x}$$

where

x = axial direction	u = axial velocity
r = radial direction	V_r = radial velocity
θ = angular direction	V_θ = tangential velocity

(See Figure 1)

Multiplying continuity by $u^2/2$ and momentum by u,

$$u\frac{\partial u}{\partial t} + u\frac{\partial}{\partial x}\left(\frac{u^2}{2}\right) + V_r\frac{\partial}{\partial r}\left(\frac{u^2}{2}\right) = -\frac{u}{\rho}\frac{\partial P}{\partial x} \qquad (1)$$

$$\frac{1}{r}\left(\frac{u^2}{2}\right)\frac{\partial}{\partial r}(r V_r) + \frac{u^2}{2}\frac{\partial u}{\partial x} \qquad (2)$$

Adding (1) and (2) to other,

$$\frac{\partial}{\partial t}\left(\frac{u^2}{2}\right) + \left[u\frac{\partial}{\partial x}\left(\frac{u^2}{2}\right) + \frac{u^2}{2}\frac{\partial u}{\partial x}\right] + \frac{1}{r}\left[(rV_r)\frac{\partial}{\partial r}\left(\frac{u^2}{2}\right) + \frac{u^2}{2}\frac{\partial (rV_r)}{\partial r}\right]$$
$$= -\frac{u}{\rho}\frac{\partial P}{\partial x} \tag{3}$$

Simplifying by combining terms in each bracket,

$$\frac{\partial}{\partial t}\left(\frac{u^2}{2}\right) + \frac{\partial}{\partial x}\left(u\frac{u^2}{2}\right) + \frac{1}{r}\frac{\partial}{\partial r}\left(rV_r\frac{u^2}{2}\right) = -\frac{u}{\rho}\frac{\partial P}{\partial x} \tag{4}$$

Since the flow is axially-symmetric, the flow passage cross-section is always circular. Then:

$$dA = 2\pi r\,dr$$

Multiplying (4) through by dA and integrating with respect to r,

$$\int_A \frac{\partial}{\partial t}\left(\frac{u^2}{2}\right)dA + \int_A \frac{\partial}{\partial x}\left(u\frac{u^2}{2}\right)dA + \int_0^R 2\pi\frac{\partial}{\partial r}\left(rV_r\frac{u^2}{2}\right)dr = -\int_A \frac{u}{\rho}\frac{\partial P}{\partial x}dA \tag{5}$$

Now, assume that the flow across any cross-section is such that u is a function only of axial position of that section and not of distance from the axis; i.e., the axial velocity is uniform across any section. Then:

$$u = u(x,t) \quad \text{only, and} \quad \frac{\partial}{\partial t}\left(\frac{u^2}{2}\right) = \text{function of } (x,t) \text{ only.}$$

Introducing this condition into (5) and integrating gives:

$$\frac{\partial}{\partial t}\left(\frac{u^2}{2}\right)A + \frac{\partial}{\partial x}\left(u\frac{u^2}{2}\right)A + 2\pi\left[rV_r\right]_0^R\left(\frac{u^2}{2}\right) = -\frac{u}{\rho}\int_0^R 2\pi r\frac{\partial P}{\partial x}dr \tag{6}$$

To evaluate (rV_r) at $r = 0$ and $r = R$ (the wall of the containing vessel), consider the following boundary conditions:

At $r = 0$, $V_r = 0$ — to satisfy axial symmetry, no fluid crosses central streamline

At $r = R$, V_r/u is tangent to fluid passage wall, hence:

$$\frac{V_r}{u} = \frac{dR}{dx}$$

The third term of (6) then becomes:

$$2\pi\left(\frac{u^2}{2}\right)\left(uR\frac{dR}{dx} - 0\right) = u\left(2\pi R\frac{dR}{dx}\right)\frac{u^2}{2} = u\frac{u^2}{2}\frac{dA}{dx} \qquad (7)$$

(Note: Since R depends upon x and not t, $\frac{dR}{dx} = \frac{\partial R}{\partial x}$ and $\frac{dA}{dx} = \frac{\partial A}{\partial x}$)

Introducing (7) into (6),

$$A\frac{\partial}{\partial t}\left(\frac{u^2}{2}\right) + A\frac{\partial}{\partial x}\left(u\frac{u^2}{2}\right) + u\frac{u^2}{2}\frac{\partial A}{\partial x} = -\frac{u}{\rho}\int_0^R \frac{\partial p}{\partial x}2\pi r\,dr$$

Combining the 2nd and 3rd terms,

$$A\frac{\partial}{\partial t}\left(\frac{u^2}{2}\right) + \frac{\partial}{\partial x}\left(uA\frac{u^2}{2}\right) = -\frac{u}{\rho}\int_0^{\pi R^2}\frac{\partial p}{\partial x}\,dA \qquad (8)$$

In order to evaluate (8) it becomes necessary to specify $p(r, x)$ and introduce its values at the limits.

Referring to Figure 1, assume $V_r << V_\theta$, so that the influence of V_r upon the radial pressure gradient is negligible. Also assume the velocity in any plane normal to the axis is such that the tangential component satisfies the conditions of an irrotational vortex. That is

$$\frac{V_\theta}{V_{\theta_e}} = \frac{R}{r}$$

, where subscript e refers to the exterior streamline at any section, i.e., $V_{\theta_e} = V_\theta$ at $r = R$.

From centrifugal force considerations, the radial pressure variation may be expressed as:

$$\frac{\partial P}{\partial r} = \rho \frac{V_\theta^2}{r}$$; or, substituting for $V_\theta = V_{\theta_e}\frac{R}{r}$,

$$\frac{\partial P}{\partial r} = \frac{\rho V_{\theta_e}^2 R^2}{r^3}$$

Integrating with respect to r,

$$\frac{P_e - P}{\rho} = \frac{V_{\theta_e}^2}{2}\left(\frac{R^2}{r^2} - 1\right)$$

or,

$$P = P_e - \frac{\rho V_{\theta_e}^2}{2}\left(\frac{R^2}{r^2} - 1\right) \qquad (9)$$

From this expression it appears that p becomes infinite in the negative sense when r approaches zero. Since this is physically impossible, we will limit this expression for p to such values of radius as reduce the pressure to the vaper pressure of the fluid under consideration. (Note that this is in accord with the assumption of incompressibility of the fluid.) Within the cavitating core, then, the pressure may vary between this vapor pressure and zero. This variation of pressure may now be substituted into the integral expression given in (8). Thus

$$\int_0^{\pi R^2} \frac{\partial P}{\partial x} dA = \int_0^{\pi R_0^2} \frac{\partial P}{\partial x} dA + \int_{\pi R_0^2}^{\pi R^2} \frac{\partial}{\partial x}\left[P_e - \frac{\rho V_{\theta_e}^2}{2}\left(\frac{R^2}{r^2} - 1\right)\right] dA \qquad (10)$$

Applying Leibnis's rule to these integrals gives:

$$\int_0^{\pi R^2} \frac{\partial P}{\partial x} dA = \frac{\partial}{\partial x}\int_0^{\pi R_0^2} P\, dA + P(0,x)\frac{d(0)}{dx} - P(R_0,x)\frac{d(\pi R_0^2)}{dx}$$

$$+ \frac{\partial}{\partial x}\int_{\pi R_0^2}^{\pi R^2}\left[P_e - \frac{\rho V_{\theta_e}^2}{2}\left(\frac{R^2}{r^2} - 1\right)\right] dA + P(R_0,x)\frac{d(\pi R_0^2)}{dx} - P(R,x)\frac{d(\pi R^2)}{dx}$$

Now, since p must remain finite or zero even at zero radius, the term $p(0, x)\frac{d(0)}{dx} = 0$. Then:

$$\int_0^{\pi R^2}\frac{\partial p}{\partial x}dA = \frac{\partial}{\partial x}\int_0^{\pi R^2} P\,dA + \frac{\partial}{\partial x}\int_{\pi R_0^2}^{\pi R^2}\left[P_e - \frac{\rho V_{\theta_e}^2}{2}\left(\frac{R^2}{r^2}-1\right)\right]dA - P_e(x)\frac{dA}{dx} \quad (11)$$

Since the accurate variation of pressure between R = 0 and R = Ro is not known and is not readily susceptible to analysis, it must be approximated. As previously noted, this is the region of cavitation of the fluid within the flow passage; therefore, it will be assumed that the pressure throughout this entire region is equal to the vapor pressure of the fluid. (Note that this gives the maximum possible value to the integral term, since the pressure must lie somewhere between vapor pressure and zero.) Equation (11) then becomes:

$$\int_0^{\pi R^2}\frac{\partial p}{\partial x}dA = \frac{\partial}{\partial x}(P_v A_0) - P_e\frac{dA}{dx} + \frac{\partial}{\partial x}\int_{A_0}^{A} P_e\,dA - \frac{\partial}{\partial x}\left[\frac{\rho V_{\theta_e}^2}{2}\int_{\pi R_0^2}^{\pi R^2}\left(\frac{R^2}{r^2}-1\right)dA\right]$$

$$= P_v\frac{dA_0}{dx} - P_e\frac{dA}{dx} + \frac{\partial}{\partial x}\left[P_e(A-A_0)\right] - \frac{\partial}{\partial x}\left[\rho V_{\theta_e}^2(\pi R^2)\int_{R_0}^{R}\frac{dr}{r}\right] + \frac{\partial}{\partial x}\left[\frac{\rho V_{\theta_e}^2}{2}\int_{A_0}^{A}dA\right]$$

$$= P_v\frac{dA_0}{dx} - P_e\frac{dA}{dx} + P_e\frac{d(A-A_0)}{dx} + (A-A_0)\frac{dP_e}{dx} - \frac{\partial}{\partial x}\left(\rho V_{\theta_e}^2 A\log_e\frac{R}{R_0}\right)$$

$$+ \frac{\partial}{\partial x}\left[\frac{\rho V_{\theta_e}^2}{2}(A-A_0)\right]$$

or

$$\int_0^{A}\frac{\partial P}{\partial x}dA = P_v\frac{dA_0}{dx} - P_e\frac{dA_0}{dx} + (A-A_0)\frac{dP_e}{dx} - \left(\rho A V_{\theta_e}^2\right)\frac{\partial}{\partial x}\left(\log_e\frac{R}{R_0}\right)$$

$$- \log_e\frac{R}{R_0}\frac{\partial}{\partial x}\left(\rho A V_{\theta_e}^2\right) + \frac{\rho V_{\theta_e}^2}{2}\frac{d}{dx}(A_1-A_0) + (A-A_0)\frac{\partial}{\partial x}\left(\frac{\rho V_{\theta_e}^2}{2}\right) \quad (12)$$

Now, let us consider the variation of $AV_{\theta_e}^2$ along the passage through the vanes, from section (0) to (1) (referring to Figure 1).

$$V_{\theta_e} = u \tan\eta, \text{ where } \eta = \text{angle between the vanes and the centerline}$$

then:

$$AV_{\theta_e}^2 = \pi R_1^2 u_1 \tan^2\eta = \text{constant.}$$

From (1) to (1)', this condition is also true, since $R = R_1$ = constant. From (1)' to (2), where the cross-section changes, it is necessary that angular momentum be conserved, since no solid bodies exist within the stream to change this momentum. Thus

$$\dot{m} R V_{\theta_e} = H = \text{angular momentum} = \text{constant}$$

But

$$H = \int_0^R (\rho u) r V_\theta (2\pi r\, dr)$$

, which (since it is a constant) may be evaluated at section (1), giving

$$H = \dot{m} R_1 u_1 \tan\eta$$

Thus

$$\dot{m}(R V_{\theta_e}) = \dot{m} R_1 u_1 \tan\eta$$

and

$$\left(AV_{\theta_e}^2\right)_{(1)'-(2)} = \pi R_1^2 u_1^2 \tan^2\eta = \text{constant.}$$

Therefore $\frac{\partial}{\partial x}\left(\frac{\rho A V_{\theta_e}^2}{2}\right)_{(0)-(2)} = 0$, and Equation (12) becomes:

$$\int_0^{\pi R^2} \frac{\partial P}{\partial x} dA = (P_v - P_e)\frac{dA_0}{dx} + (A - A_0)\frac{dP_e}{dx} - \left(\frac{\rho A V_{\theta_e}^2}{2}\right)\frac{d}{dx}\left(\log_e \frac{A}{A_0}\right) + \frac{\rho V_{\theta_e}^2}{2}\frac{d}{dx}(A - A_0)$$
$$+ (A - A_0)\frac{d}{dx}\left(\frac{\rho V_{\theta_e}^2}{2}\right)$$

$$= (P_v - P_e)\frac{dA_o}{dx} + (A - A_o)\left[\frac{dP_e}{dx} + \frac{d}{dx}\left(\frac{\rho V_{\theta_e}^2}{2}\right)\right] - \frac{\rho A V_{\theta_e}^2}{2}\frac{d}{dx}\left(\log_e A - \log_e A_o\right)$$

$$+ \frac{\rho V_{\theta_e}^2}{2}\left(\frac{dA}{dx} - \frac{dA_o}{dx}\right)$$

$$= (P_v - P_e)\frac{dA_o}{dx} + (A - A_o)\frac{d}{dx}\left(P_e + \frac{\rho V_{\theta_e}^2}{2}\right) - \frac{\rho A V_{\theta_e}^2}{2}\left(\frac{1}{A}\frac{dA}{dx} - \frac{1}{A_o}\frac{dA_o}{dx}\right)$$

$$+ \frac{\rho V_{\theta_e}^2}{2}\frac{dA}{dx} - \frac{\rho V_{\theta_e}^2}{2}\frac{dA_o}{dx}$$

$$= (P_v - P_e)\frac{dA_o}{dx} - \frac{\rho V_{\theta_e}^2}{2}\frac{dA}{dx} + \frac{\rho V_{\theta_e}^2}{2}\left(\frac{A}{A_o}\right)\frac{dA_o}{dx} + \rho\frac{V_{\theta_e}^2}{2}\frac{dA}{dx} - \frac{\rho V_{\theta_e}^2}{2}\frac{dA_o}{dx}$$

$$+ (A - A_o)\frac{d}{dx}\left(P_e + \frac{\rho V_{\theta_e}^2}{2}\right)$$

$$\int_0^{\pi R^2}\frac{\partial P}{\partial x}dA = \left[P_v - P_e + \frac{\rho V_{\theta_e}^2}{2}\left(\frac{A}{A_o} - 1\right)\right]\frac{dA_o}{dx} + (A - A_o)\frac{d}{dx}\left(P_e + \frac{\rho V_{\theta_e}^2}{2}\right) \qquad (13)$$

But, from the pressure distribution equation (equation 9),

$$P_v = P_e - \frac{\rho V_{\theta_e}^2}{2}\left(\frac{R^2}{R_o^2} - 1\right) = P_e - \frac{\rho V_{\theta_e}^2}{2}\left(\frac{A}{A_o} - 1\right)$$

Hence, the first term of Equation (13) is zero, and this equation becomes:

$$\int_0^{\pi R^2}\frac{\partial P}{\partial x}dA = A\left(1 - \frac{A_o}{A}\right)\frac{d}{dx}\left(P_e + \frac{\rho V_{\theta_e}^2}{2}\right) \qquad (14)$$

Values of Ro have been calculated for the monopropellant injectors with water as the calibrating fluid and these are approximately (referring to Figure 1),

From section (1) to (1^1):

$R^2 = R_1^2 = .01612\ in^2$

$R_o^2 = 4.37 \times 10^{-6} in^2$ to $12.32 \times 10^{-6} in^2$

for the range of main flows from 1.0 #/sec. to 3.0 #/sec.

From (1^1) to (2):

$$R^2 = .01451 \text{ to } .001679 \text{ in}^2$$

$$R_o^2 = 4.42 \times 10^{-6} \text{ (min. at large R)}$$

$$\text{to: } 9.78 \times 10^{-6} \text{ (max. at small R)}$$

Hence:

From (1) to (1^1):

$$\frac{R_o^2}{R^2} = 0.0002 \text{ to } 0.0008$$

From (1^1) to (2)

$$\frac{R_o^2}{R^2} = .0003 \text{ to } .006$$

Hence, for all practical values encountered, $R_o^2/R^2 = Ao/A <<< 1$ and may be neglected. Then, Equation (14) becomes:

$$\int_0^{\pi R^2} \frac{\partial p}{\partial x} dA \doteq A \frac{d}{dx}\left(P_e + \frac{\rho V_{\theta e}^2}{2}\right)$$

Substituting this into the original unsteady Equation (8),

$$A \frac{\partial}{\partial t}\left(\frac{U^2}{2}\right) + \frac{\partial}{\partial x}\left(UA\frac{U^2}{2}\right) = -\frac{(UA)}{\rho}\frac{\partial}{\partial x}\left(P_e + \frac{\rho V_{\theta e}^2}{2}\right)$$

But $\rho U A = \dot{m}$ = constant, with respect to x; hence,

$$\frac{\partial}{\partial t}\left(\rho A \frac{U^2}{2}\right) + \frac{\partial}{\partial x}\left(\rho U A \frac{U^2}{2}\right) + \frac{\partial}{\partial x}\left[(\rho U A)\left(\frac{P_e}{\rho} + \frac{V_{\theta e}^2}{2}\right)\right] = 0$$

$$\text{or} \quad \frac{\partial}{\partial t}\left(\rho A \frac{U^2}{2}\right) + \dot{m}\frac{\partial}{\partial x}\left(\frac{U^2 + V_{\theta e}^2}{2} + \frac{P_e}{\rho}\right) = 0 \qquad (15)$$

Integrating with respect to x between entrance and exit sections,

$$\int_1^2 \frac{\partial}{\partial t}\left(\rho A \frac{U^2}{2}\right) dx + \dot{m}\left[\frac{U^2 + V_{\theta e}^2}{2} + \frac{P_e}{\rho}\right]_1^2 = 0 .$$

$$\frac{\partial}{\partial t}\int_1^2\left(\frac{U^2}{2}\right)\rho A\,dx + \dot{m}\left[\left(\frac{W_e^2}{2}\right)_2 - \left(\frac{W_e^2}{2}\right)_1 + \frac{P_{e_2}-P_{e_1}}{\rho}\right] = 0 \qquad (16)$$

where: $W_e = \sqrt{U^2 + V_{\theta_e}^2}$ = total velocity vector

at $r = R$ by virtue of the fact that u = constant across any section and $V_r <<< V_\theta$.

Note that $\frac{W_e^2}{2}$ is the kinetic energy per unit mass of fluid at the exterior streamline of the flow, which we may designate as $\mathcal{E}$.

Also note that $\rho A dx\left(\frac{U^2}{2}\right)$ is the elemental portion of the kinetic energy contribution of the x-directed velocity. If we designate this as dE_x, we may write a final form of equation (16) as:

$$\frac{\partial}{\partial t}\int_1^2 dE_x + \dot{m}(\mathcal{E}_2-\mathcal{E}_1) + \frac{\dot{m}}{\rho}(P_{e_2}-P_{e_1}) = 0$$

or:

$$\frac{\partial E_x}{\partial t} + \dot{m}(\mathcal{E}_2-\mathcal{E}_1) = \frac{\dot{m}}{\rho}(P_{e_1}-P_{e_2}) = \frac{\dot{m}}{\rho}\Delta P_e$$

or, finally:

$$\Delta P_e = \frac{\rho}{\dot{m}}\frac{\partial E_x}{\partial t} + \rho(\mathcal{E}_2-\mathcal{E}_1) \qquad (17)$$

It is now relatively simple to examine the behavior of ΔP_e in the case of unsteady flows where the variation from steady flow conditions may be treated as a small perturbation. For example, let:

$$\dot{m} = \bar{\dot{m}}(1+\mu) \qquad \text{and} \qquad \Delta P_e = \overline{\Delta P_e}(1+\psi)$$

where the bar denotes steady-state conditions.

Then

$$U = \frac{\dot{m}}{\rho A} = \frac{\bar{\dot{m}}}{\rho A}(1+\mu) = \bar{U}(1+\mu)$$

and

$$V_{\theta_e} = \left(\frac{R_1}{R}\right)U_1\tan\eta = KU_1 = K\bar{U}_1(1+\mu) = \bar{V}_{\theta_e}(1+\mu)$$

Then
$$\mathcal{E} = \frac{U^2 + V_{\theta_2}^2}{2} = \frac{\overline{U}^2(1+\mu)^2 + \overline{V}_{\theta_2}^2(1+\mu)^2}{2}$$
$$= \frac{\overline{U}^2 + \overline{V}_{\theta_2}^2}{2}(1+\mu)^2 = (1+\mu)^2\,\overline{\mathcal{E}}$$

and
$$E_x = \int_1^2 \rho A \frac{\overline{U}^2}{2}(1+\mu)^2\,dx$$

Now, note that since μ represents a fractional change of mass flow and/or velocity, it is dependent upon time only, and not upon axial position, x.

Hence:
$$E_x = (1+\mu)^2\int_1^2\left(\frac{\overline{U}^2}{2}\right)\rho A\,dx = (1+\mu)^2\,\overline{E}_x$$

However, $\overline{E}_x$ is a steady-state parameter and independent of time.

Therefore:
$$\frac{\partial}{\partial t}(E_x) = \overline{E}_x\frac{\partial}{\partial t}(1+\mu)^2$$

Substituting these perturbation quantities into Equation (17),
$$\overline{\Delta P}_e(1+\psi) = \frac{\rho\overline{E}_x}{\overline{m}(1+\mu)}\frac{\partial}{\partial t}(1+\mu)^2 + \rho(1+\mu)^2(\overline{\mathcal{E}}_2-\overline{\mathcal{E}}_1)$$
or:
$$\overline{\Delta P}_e(1+\psi) = \frac{\rho\overline{E}_x}{\overline{m}}2\frac{\partial\mu}{\partial t} + \rho(1+2\mu+\mu^2)(\overline{\mathcal{E}}_2-\overline{\mathcal{E}}_1)$$
or, neglecting μ^2 in comparison with μ and $\frac{\partial\mu}{\partial t}$,

$$\psi\,\overline{\Delta P}_e = \frac{2\rho\overline{E}_x}{\overline{m}}\frac{\partial\mu}{\partial t} + 2\rho\mu(\overline{\mathcal{E}}_2-\overline{\mathcal{E}}_1) + \left[\rho(\overline{\mathcal{E}}_2-\overline{\mathcal{E}}_1) - \Delta P_e\right] \quad (18)$$

But, from Equation (17), when there are no time variations, i.e., under steady state conditions,
$$\overline{\Delta P}_e = \rho(\overline{\mathcal{E}}_2-\overline{\mathcal{E}}_1)$$

Making this substitution in (18) gives
$$\rho\psi(\overline{\mathcal{E}}_2-\overline{\mathcal{E}}_1) = \frac{2\rho\overline{E}_x}{\overline{m}}\frac{\partial\mu}{\partial t} + 2\rho\mu(\overline{\mathcal{E}}_2-\overline{\mathcal{E}}_1)$$

or:

$$\psi = \left[\frac{2\bar{E}_x}{\bar{\dot{m}}(\bar{\mathcal{E}}_2 - \bar{\mathcal{E}}_1)}\right]\frac{\partial\mu}{\partial t} + 2\mu \tag{19}$$

Grouping the constants of the first term of (19) together into one constant, σ, we have:

$$\psi = 2\mu + \sigma\frac{\partial\mu}{\partial t} \tag{20}$$

To approximate the conditions of oscillatory flow in the monopropellant system, let: $\mu = \tilde{\mu}e^{i\omega t}$

and: $\dfrac{\partial\mu}{\partial t} = i\omega\tilde{\mu}e^{i\omega t} = i\omega\mu$.

Then $\psi = 2\mu + i\omega\sigma\mu = 2\mu\left(1 + \dfrac{i\omega\sigma}{2}\right)$

Now, let $\alpha = \tan^{-1}\dfrac{\omega\sigma}{2}$

Then

$$1 + \frac{i\omega\sigma}{2} = 1 + i\tan\alpha = 1 + \frac{i\sin\alpha}{\cos\alpha}$$

$$= \frac{\cos\alpha + i\sin\alpha}{\cos\alpha} = \frac{e^{i\alpha}}{\cos\alpha}$$

Then Equation (20) becomes:

$$\underline{\psi = \left(\frac{2}{\cos\alpha}\right)\mu e^{i\alpha}} \tag{21}$$

where the symbols employed are as follows:

$$\psi = \frac{\Delta P_e - \overline{\Delta P_e}}{\overline{\Delta P_e}} \qquad \bar{E}_x = \int_1^2 \left(\frac{\bar{U}^2}{2}\right)\rho A\,dx$$

$$\mu = \frac{\dot{m} - \bar{\dot{m}}}{\bar{\dot{m}}} = \frac{U - \bar{U}}{\bar{U}} \qquad \bar{\mathcal{E}} = \frac{\bar{U}^2 + \bar{V}_{\theta_e}^2}{2}$$

$$\alpha = \tan^{-1}\frac{\omega\sigma}{2} \qquad \bar{V}_{\theta_e} = \left(\frac{R_1}{R}\right)\bar{U}_1\tan\eta$$

$$\sigma = \frac{2\bar{E}_x}{\bar{\dot{m}}(\bar{\mathcal{E}}_2 - \bar{\mathcal{E}}_1)} \qquad \eta = \text{angle between vanes and axis of flow passage}$$

It is now possible, for various flow conditions, to calculate numerical values for α based on the above approximations.

Thus $$\bar{E}_1 = \frac{\bar{U}_1^2 + \bar{V}_{\theta_{e_1}}^2}{2} = \frac{\bar{U}_1^2}{2}$$ (since $\bar{V}_{\theta_{e_1}} = 0$, $\eta = 0$ before entrance to vanes)

and $$\bar{E}_2 = \frac{\bar{U}_2^2 + \bar{V}_{\theta_{e_2}}^2}{2} = \frac{\bar{U}_2^2 + \bar{U}_1^2 \frac{R_1^2}{R_2^2} \tan^2 \eta}{2}$$

But: $$\bar{U}_1 A_1 = \bar{U}_2 A_2$$ (since $\dot{m}$ = constant and ρ = constant)

or: $$\bar{U}_2 = \bar{U}_1 \frac{A_1}{A_2} = \bar{U}_1 \frac{R_1^2}{R_2^2}; \qquad \bar{U}_2^2 = \bar{U}_1^2 \frac{R_1^4}{R_2^4}$$

Thus $$\bar{E}_2 = \frac{\bar{U}_1^2}{2}\left(\frac{R_1^2}{R_2^2}\right)\left(\frac{R_1^2}{R_2^2} + \tan^2 \eta\right)$$

and $$\bar{E}_2 - \bar{E}_1 = \frac{\bar{U}_1^2}{2}\left[\left(\frac{R_1}{R_2}\right)^2\left(\frac{R_1^2}{R_2^2} + \tan^2 \eta\right) - 1\right]$$

To evaluate E_2, the variation of R with x must be known. From approximate measurements (referring to Figures 1 and 2), this has been found to be of the form:

$$R = R_1 = \text{constant from } x = 0 \text{ to } x = \ell_1$$

$$\text{and } R = R_2 = \text{constant from } x = \ell_2 \text{ to } x = \ell$$

From $x = \ell_1$ to $x = \ell_2$, $(R+h)^2 + (x-\ell_1)^2 = S^2$

or: $$(R+h)^2 = S^2 - \xi^2, \qquad \text{where } \xi = x - \ell_1$$

$$R + h = \sqrt{S^2 - \xi^2}$$

$$R = \sqrt{S^2 - \xi^2} - h$$

Now: $\frac{\bar{U}}{\bar{U}_1} = \frac{A_1}{A} = \frac{R_1^2}{R^2}$

or: $\bar{U} = \bar{U}_1 R_1^2 / (\sqrt{S^2 - \xi^2} - h)^2$

Now, $\bar{E}_x = \int_1^2 \frac{\bar{U}^2}{2} \rho A dx = \int_1^2 (\rho \bar{U} A) \frac{\bar{U}}{2} dx = \bar{\dot{m}} \int_1^2 \frac{\bar{U} dx}{2}$

This integral may be evaluated in three parts:

$$\bar{E}_x = \bar{\dot{m}} \int_1^{1'} \frac{\bar{U}}{2} dx + \bar{\dot{m}} \int_{1'}^{2'} \frac{\bar{U}}{2} dx + \bar{\dot{m}} \int_{2'}^{2} \frac{\bar{U}}{2} dx$$

The first and last of these may be evaluated immediately, since $\bar{u} = \bar{u}_1$ = constant from (1) to $(1)^1$ and $\bar{u} = \bar{u}_2$ = constant from $(2)^1$ to (2).

Then:

$$E_x = \frac{\bar{\dot{m}} \bar{U}_1 l_1}{2} + \frac{\bar{\dot{m}} \bar{U}_2 (l - l_2)}{2} + \bar{\dot{m}} \int_{1'}^{2'} \frac{\bar{U}}{2} dx$$

The last integral, which we may designate as I, may be evaluated by introducing the velocity distribution analysed previously. Then

$$(E_x)_{1-2'} = \frac{\bar{\dot{m}} \bar{U}_1 R_1^2}{2} \int_0^{l_2 - l_1} \frac{d\xi}{(\sqrt{S^2 - \xi^2} - h)^2} = \frac{\bar{\dot{m}} \bar{U}_1 R_1^2}{2} I$$

This may be reduced to an integrable form by the substitution

$$z = \sqrt{S^2 - \xi^2} - h$$

then: $\xi = \sqrt{(S^2 - h^2) - 2hz - z^2}$

and: $d\xi = \frac{-(z + h) dz}{\xi}$

at: $\xi = 0$, then, $z = S - h$; and at $\xi = l_2 - l_1 = \Delta l$,

$$z = \sqrt{S^2 - (\Delta l)^2} - h = z_l$$

So:

$$I = \int_0^{\Delta l} \frac{d\xi}{\left(\sqrt{s^2-\xi^2}-h\right)^2} = \int_{s-h}^{z_2} \frac{-(z+h)\,dz}{z^2\sqrt{(s^2-h^2)-2hz-z^2}} = -\int_{s-h}^{z_2}\frac{dz}{z\,Z^{1/2}} - h\int_{s-h}^{z_2}\frac{dz}{z^2 Z^{1/2}}$$

where: $Z = az^2 + bz + c = -z^2 - 2hz + (s^2-h^2)$

Both these integral forms are tabulated, and their integrated values are:

$$I_1 = \int\frac{dz}{z\,Z^{1/2}} = -\frac{1}{\sqrt{c}}\log_e\left|\frac{2(cZ)^{1/2}}{z} + \frac{2c}{z} + b\right|$$

$$I_2 = \int\frac{dz}{z^2 Z^{1/2}} = -\frac{Z^{1/2}}{cz} - \frac{b}{2c}\left\{-\frac{1}{\sqrt{c}}\log_e\left|\frac{2(cZ)^{1/2}}{z} + \frac{2c}{z} + b\right|\right\}$$

These are subject to the condition that $c > 0$; and to investigate this requirement, a more detailed sketch of the injector flow passage between $(1)^1$ and (2) is shown in Figure 2.

Thus $\sqrt{s^2-\xi^2} = z + h$

and: $z = R$ = radius of flow passage

At: $\xi = 0, \quad s = R_1 + h, \quad z = R_1$

At: $\xi = l_2 - l_1, \quad \sqrt{s^2-\xi^2} = R_2 + h, \quad z = R_2$

Now C = constant in the expression $Z = az^2 + bz + c = (s^2 - h^2)$

So: $C > 0$ for all ξ, since $s > h$.

Therefore, the condition for integration is satisfied, and we may substitute for a, b, c, and Z and evaluate the integrals at their limits.

Thus:

$$I_1 = -\frac{1}{\sqrt{c}}\log_e\left|\frac{2(cZ)^{1/2}}{z} + \frac{2c}{z} + b\right|$$

$$= -\frac{1}{\sqrt{s^2-h^2}}\log_e\left|\frac{2\sqrt{s^2-h^2}\sqrt{-z^2-2hz+(s^2-h^2)}}{z} + \frac{2(s^2-h^2)}{z} - 2h\right|$$

$$I_2 = \frac{-Z^{1/2}}{cz} - \frac{b}{2c}(I_1)$$

$$= \frac{\sqrt{-z^2-2hz+(s^2-h^2)}}{(s^2-h^2)z} + \frac{h}{(s^2-h^2)}\left\{\frac{-1}{\sqrt{s^2-h^2}}\log_e\left|\frac{2\sqrt{s^2-h^2}\sqrt{-z^2-2hz+(s^2-h^2)}}{z} + \frac{2(s^2-h^2)}{z} - 2h\right|\right\}$$

Now, since $(s^2 - h^2)$ occurs frequently as a constant, let it have a separate symbol, say k^2, then:

$$I_1 = -\frac{1}{k}\log_e\left|\frac{2k\sqrt{-z^2-2hz+k^2}}{z} + \frac{2k^2}{z} - 2h\right|$$

$$I_2 = -\frac{\sqrt{-z^2-2hz+k^2}}{k^2 z} - \frac{h}{k^3}\log_e\left|\frac{2k\sqrt{-z^2-2hz+k^2}}{z} + \frac{2k^2}{z} - 2h\right|$$

Now $$I = -\int_{s-h}^{z_2}\frac{dz}{z Z^{1/2}} - h\int_{s-h}^{z_2}\frac{dz}{z^2 Z^{1/2}} = -I_1 - hI_2$$

Thus,

$$I = \left\{\frac{h}{k^2 z}\sqrt{-z^2-2hz+k^2} + \left(\frac{h^2}{k^3}+\frac{1}{k}\right)\log_e\left|\frac{2k\sqrt{-z^2-2hz+k^2}}{z} + \frac{2k^2}{z} - 2h\right|\right\} \qquad (22)$$

This expression may be simplified slightly by re-substituting the original variable ξ and noting that:

$$\frac{h^2}{k^3} + \frac{1}{k} = \frac{1}{k}\left(\frac{h^2+k^2}{k^2}\right) = \frac{1}{k^3}\left(h^2+s^2-h^2\right) = \frac{s^2}{k^3}$$

Also, since $z = \sqrt{s^2-\xi^2} - h$, from Figure 2, $z > 0$ for all ξ. Then $2/z = |2/z|$, and this common factor may be taken outside the absolute value sign.

Thus: $$\xi = \sqrt{s^2-(z+h)^2} = \sqrt{-z^2-2hz+s^2-h^2} = \sqrt{-z^2-2hz+k^2}$$

Hence, equation (22) becomes

$$I = \left\{\frac{h\xi}{k^2 z} + \frac{s^2}{k^3}\log_e\left[\frac{2}{z}\left|k\xi + k^2 - hz\right|\right]\right\}_{\substack{\xi=0\\ z=R_1}}^{\substack{\xi=\Delta\ell\\ z=R_2}} \qquad (23)$$

Inserting the limits in (23),

$$I = \left\{ \frac{h\Delta\ell}{k^2 R_2} - \frac{h(0)}{k^2 R_1} + \frac{s^2}{k^3} \log_e \left[\frac{2/R_2 \left(k\Delta\ell + k^2 - hR_2\right)}{2/R_1 \left(k\cdot 0 + k^2 - hR_1\right)} \right] \right\}$$

$$= \frac{h\Delta\ell}{k^2 R_2} + \frac{s^2}{k^3} \log_e \left[\frac{R_1\left(k\Delta\ell + k^2 - hR_2\right)}{R_2\, s(s-h)} \right]$$

or, finally:

$$I = \frac{h\Delta\ell}{k^2 R_2} + \frac{s^2}{k^3} \log_e \left(\frac{k\Delta\ell + k^2 - hR_2}{sR_2} \right) \tag{24}$$

(The absolute value sign is removed, since the numerator > 0.)

Then:

$$\overline{E}_x = \frac{\overline{\dot m}\,\overline{U}_1 \ell_1}{2} + \frac{\overline{\dot m}\,\overline{U}_2 (\ell - \ell_2)}{2} + I\,\frac{\overline{\dot m}\,\overline{U}_1 R_1^2}{2}$$

or:

$$\overline{E}_x = \frac{\overline{\dot m}\,\overline{U}_1}{2} \left[\ell_1 + \frac{R_1^2}{R_2^2}(\ell - \ell_2) + \frac{h(\ell_2 - \ell_1) R_1^2}{k^2 R_2} + \frac{R_1^2 s^2}{k^3} \log_e \left(\frac{k(\ell_2 - \ell_1) + k^2 - hR_2}{sR_2} \right) \right] \tag{25}$$

The next step in evaluating Equation (21) is to combine the steady-state terms to form σ. Thus:

$$\sigma = \frac{2\overline{E}_x}{\overline{\dot m}\left(\overline{E}_2 - \overline{E}_1\right)}$$

$$\sigma = \frac{\frac{2}{\overline{U}_1}\left[\ell_1 + \frac{R_1^2}{R_2^2}(\ell - \ell_2) + \frac{h(\ell_2 - \ell_1) R_1^2}{k^2 R_2} + \frac{s^2 R_1^2}{k^3} \log_e \frac{k(\ell_2 - \ell_1) + k^2 - hR_2}{sR_2} \right]}{\left(\frac{\ell_1}{R_2}\right)^2 \left(\frac{R_1^2}{R_2^2} + \tan^2 \eta \right) - 1} \tag{26}$$

From these [illegible] and from specified values of frequency and mass flow, the phase lag and amplitude ratio between injector pressure drop and flow leaving the nozzle may be computed. These calculations were performed with the following dimensions employed. Results are shown in figures 3 and 4.

$R_1 = 0.127$ in

$R_2 = 0.041$ in

$\eta = 55^\circ$

$\ell_1 = .3920$ in

$\ell_2 = .5201$ in

$\ell = .55935''$

$s = 5/32'' = .15625''$

$h = .03575''$